Proc. Natl. Acad. Sci. USA
Vol. 88, pp. 26–30, January 1991
Biochemistry

NMR and molecular modeling evidence for a G·A mismatch base pair in a purine-rich DNA duplex

YING LI*, GERALD ZON†, AND W. DAVID WILSON*‡

*Department of Chemistry and The Laboratory for Microbial and Biochemical Sciences, Georgia State University, Atlanta, GA 30303-3083; and †Applied Biosystems, 850 Lincoln Centre Drive, Foster City, CA 94404

Communicated by I. Tinoco, Jr., September 17, 1990

ABSTRACT **^{1}H NMR experiments indicate that the oligomer 5′-d(ATGAGCGAATA) forms an unusual 10-base-pair duplex with 4 G·A base pairs (underlined) and a 3′ unpaired adenosine. NMR results indicate that guanosine imino protons of the G·A mismatches are not hydrogen bonded but are stacked in the helix. A G → I substitution in either G·A base pair causes a dramatic decrease in duplex stability and indicates that hydrogen bonding of the guanosine amino group is critical. Nuclear Overhauser effect spectroscopy (NOESY) and two-dimensional correlated spectroscopy (COSY) results indicate that the overall duplex conformation is in the B-family. Cross-strand NOEs in two-dimensional NOESY spectra between a mismatched AH2 and an AH1′ of the other mismatched base pair and between a mismatched GH8 and GNH1 of the other mismatch establish a purine–purine stacking pattern, adenosine over adenosine and guanosine over guanosine, which strongly stabilizes the duplex. A computer graphics molecular model of the unusual duplex was constructed with G·A base pairs containing A-NH_2 to GN3 and G-NH_2 to AN7 hydrogen bonds and B-form base pairs on both sides of the G·A pairs [5′-d(ATGAGC)]. The energy-minimized duplex satisfies all experimental constraints from NOESY and COSY results. A hydrogen bond from G-NH_2 of the mismatch to a phosphate oxygen is predicted.**

Mismatches in DNA can arise, for example, in specific structures such as telomeres (1, 2), during replication, and in genetic recombination. If not corrected, the mismatches may lead to point mutations in subsequent replication (3–7). G·A mismatches are of particular interest because they are a common structural element in RNA folding (8–11). Early studies have shown that a single G·A mismatch could be readily incorporated into DNA helices and the G·A mismatch was resistant to single-strand nucleases (12, 13). In neutral aqueous buffer with the normal base tautomers, there are four types of G·A mismatch base pairs (14), and these can be grouped by imino (Fig. 1, structures A and B) or amino hydrogen bond (Fig. 1, structures C and D) pairs with respect to guanosine. Several structural studies by single-crystal x-ray diffraction and NMR methods have shown that G·A mismatches are conformationally variable. Base pairs of types A and B but not C and D have been observed (7, 15–20).

In studies of the interaction of antisense oligonucleotides with 11-base analogs of ras p21 mRNA (21), we discovered a sequence, termed 2C, 5′-d(ATGAGCGAATA), that formed an unusually stable duplex (22). Eight of 11 bases in sequence 2C are purines and, from base-pairing possibilities, an unusual duplex with four G·A mismatch base pairs was proposed for this sequence (Fig. 2*a*) (22). We have undertaken NMR studies to define this unusual duplex in more detail and report here the observations of G·A mismatches of type D and unusual purine·purine base stacking in a B-form duplex.

The publication costs of this article were defrayed in part by page charge payment. This article must therefore be hereby marked "*advertisement*" in accordance with 18 U.S.C. §1734 solely to indicate this fact.

MATERIALS AND METHODS

Oligonucleotides were synthesized as described (22). NMR experiments were performed on a Varian VXR 400 NMR spectrometer. Oligomer strands were dissolved at 2 mM in 0.5 ml of buffer in a 5-mm NMR tube. Pipes buffer (10 mM Pipes/1 mM EDTA/0.2 M NaCl, pH 6.8) with a $^2H_2O/^1H_2O$ molar ratio of 1:9 and phosphate buffer (7.5 mM NaH_2PO_4/0.1 mM EDTA/0.2 M NaCl, pH 6.8) with 99.96% ^2H_2O were used for exchangeable and nonexchangeable ^1H NMR studies, respectively. Phase-sensitive nuclear Overhauser effect spectroscopy (NOESY) spectra with mixing times from 50 to 300 ms were recorded with 1024 data points in the t_2 dimension, 64–96 acquisitions per t_1 increment, 256 increments in the t_1 dimension zero-filling to 1024 data points. Absolute-mode two-dimensional correlated spectroscopy (COSY) spectra were recorded with 512 increments in the t_1 dimension zero-filling to 1024 data points. The sweep width was about 3500 Hz with a repetition delay of 1 or 1.5 s. Free induction decays (FIDs) were apodized with a shifted-sine bell function for NOESY and non-shifted-sine bell function for COSY before Fourier transforming.

$^1H/^2H$ exchange experiments were undertaken inside an NMR tube. Oligomer DNA was heated at 90°C in ^2H_2O buffer. Once every hour the samples were cooled down for NMR spectra until 90% of the GH8 was exchanged (3–4 hr).

One-dimensional (1D) exchangeable proton NMR spectra were obtained using either the 1-1 or the 1-3-3-1 solvent suppression pulse sequence (23) with the carrier frequency set at the water resonance. The sweep width varied from 8000 to 10,000 Hz with a 1-s recycle delay. 1D nuclear Overhauser effect (NOE) difference spectra for imino proton assignment were obtained by alternately placing the decoupler on and off imino proton resonances of interest. Sodium 3-(trimethylsilyl)propionate-*2,2,3,3-d*$_4$ was used as internal reference for all the experiments.

Molecular modeling was conducted with the program MACROMODEL from Clark Still (24) and energy minimizations were conducted to a rms gradient of <0.1 kcal/Å (1 cal = 4.184 J) with the force field developed by Kollman and coworkers (25). Since sequence 2C has a C2 symmetry axis at the G(5)C(6) position (see below) modeling was conducted on the hexamer sequence d[A(1)T(2)G(3)A(4)G(5)C(6)]·d[G(5)C(6)G(7)A(8)A(9)T(10)]. Models of either types C and D base pairs were first constructed and were joined to form the adjacent mismatched base pairs. Normal B-form AT and GC sequences were constructed and joined to the 5′ and 3′ ends, respectively, of the GA sequence. The units were connected to create the minimum possible distortion in standard bond lengths and angles and to keep torsional angles as close as possible to the standard B-form range.

Abbreviations: NOE, nuclear Overhauser effect; NOESY, NOE spectroscopy; COSY, two-dimensional correlated spectroscopy; FID, free induction decay; 1D and 2D, one and two dimensional, respectively.

‡To whom reprint requests should be addressed.

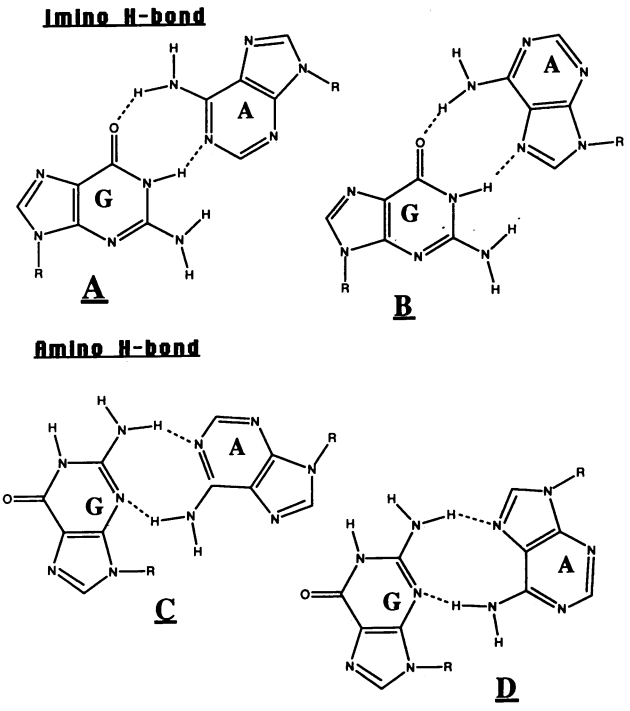

FIG. 1. Four possible G·A mismatches with the normal base tautomers, types A–D.

RESULTS AND DISCUSSION

Base Pairing in the Duplex. The proposed 2C duplex is shown in Fig. 2*a*. The duplex has C2 symmetry with four G·A mismatches, six Watson–Crick base pairs (four A·T and two G·C), and an unpaired adenosine at each end of the duplex. If this base pairing is correct, the C2 symmetry will simplify the NMR spectra and only five imino proton peaks should be seen. Fig. 2*a* shows the predicted five imino proton signals. Three of the signals are located in the normal hydrogen-bonded imino proton region (12–14 ppm), and the other two are upfield (10.4 and 10.5 ppm). NOE and temperature results were used for assignments. For example, peak 10 (Fig. 2) broadens first when the temperature is increased or the pH is raised because of end-base-pair fraying. The NOE between peaks 10 and 2 provided the assignment for the imino proton of T(2)·A(9). The mutual NOEs between peaks 7 and 5 located the G(7) and G(5)·C(6) imino proton resonances. The unique NOE at peak 5 when irradiating peak 7 indicates that peaks 7 and 3 can be independently excited even though they are partially overlapped. Peak 5 persists to high temperature confirming its assignment to the central G(5)·C(6) base pair. The base-pairing scheme in Fig. 2*a* also predicts that removal of A(11) would leave an essentially unmodified imino proton spectrum and that is observed with the 10-mer duplex 5′-d(ATGAGCGAAT), sequence 2C-10.

G·A Base-Pairing Type. The imino proton results demonstrate that the 2C duplex exists with C2 symmetry and four G·A mismatches, but they do not specify the type of G·A mismatches. The G·A guanosine imino protons in 2C resonate in an upfield region where unpaired guanosine imino proton signals are located. An unpaired guanosine imino proton could occur at the G·A mismatch site if the guanosine and adenosine bases of the mismatch are looped out of the duplex or if a base pair is formed that does not involve the guanosine imino proton. If the bases are looped out or are of types A or B (Fig. 1), a G → I substitution should have little effect on duplex stability. A G → I substitution in oligomers 2C-I1 and 2C-I2 (sequences shown in Fig. 2 *c* and *d*) lowers the melting temperature by >40°C so that complete melting curves cannot be obtained by UV absorbance. The two imino proton peaks for the mismatched base pairs also disappear from spectra of the inosine duplexes under normal NMR conditions. Lowering temperature and increasing salt concentration helps stabilize the duplexes (26), and, at −5°C, pH 5.6, and 1 M NaCl, the two missing peaks for sequence 2C-I1 become visible (Fig. 2*e*). In the inosine duplexes, the remaining mismatched guanosine imino proton signal is located at 10.5 ppm, as in sequence 2C, and the mismatched inosine imino proton is located at 12.3

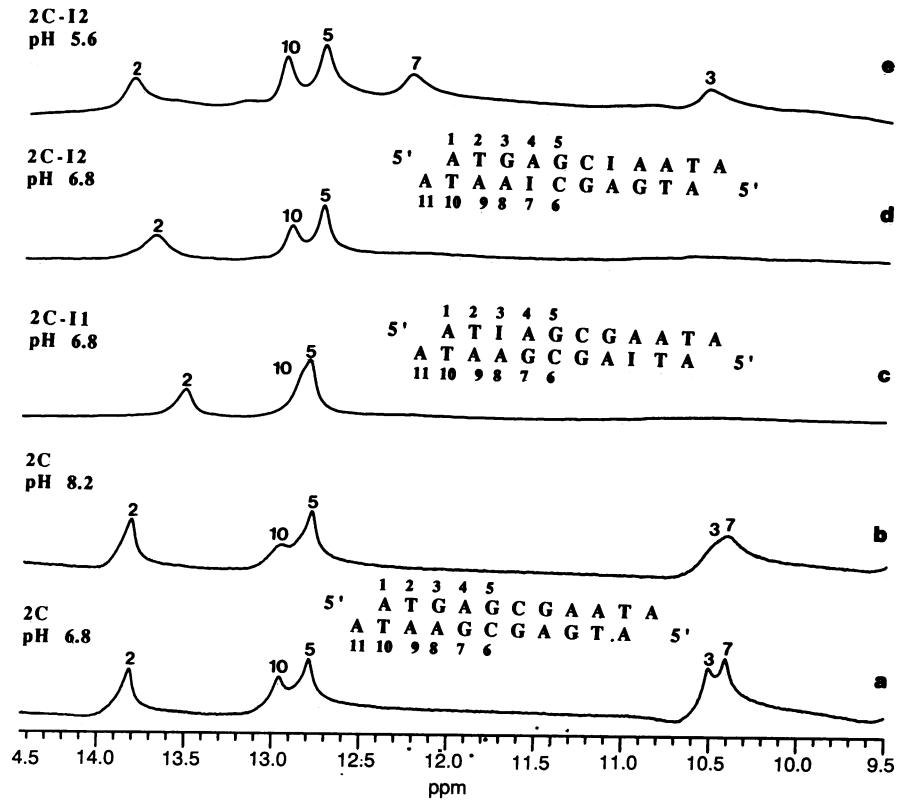

FIG. 2. Imino proton NMR spectra of sequence 2C at pH 6.8, 0°C, and 0.2 M NaCl (*a*); sequence 2C at pH 8.2, 0°C, and 0.2 M NaCl (*b*); sequence 2C-I1 at pH 6.8, 0°C, and 0.2 M NaCl (*c*); sequence 2C-I2 at pH 6.8, 0°C, and 0.2 M NaCl (*d*); and sequence 2C-I2 at pH 5.6, −5°C, and 1 M NaCl (*e*). The oligomers were in a 9:1 H_2O/^2H_2O molar solution containing 10 mM Pipes and 1 mM EDTA. Duplex sequences with base numbering for sequences 2C, 2C-I1, and 2C-I2 are shown with the spectra.

ppm, the expected imino proton region for inosine in free form or in a base pair of type C or D (27). If the imino proton of inosine is involved in an I·A base pair of type A or B, the imino signal shifts down field to near 15 ppm (28). The dramatic duplex destabilization caused by the G → I substitution and the inosine chemical shifts can be explained, however, if the mismatched base pairs are of type C or D.

The imino proton chemical shifts remain at the same positions from pH 5.5 to pH 8.2 and no new signals appear, indicting that base protonation is not involved in formation of the G·A mismatches. Raising the pH to 8.2, however, results in very significant broadening of the imino proton signals of the terminal A·T and of the two G·A mismatched base pairs (Fig. 2*b*). This indicates that the imino proton of guanosine in the G·A mismatched base pairs is much more accessible to solvent than imino protons in Watson–Crick base pairs. Clearly the imino proton has little effect, but the amino group of guanosine in the G·A base pairs plays a critical role in stabilization of the unusual duplex. Since G(3) and G(7) give very similar results in all experiments, both G·A mismatches in sequence 2C must pair in a similar way, either type C or D (Fig. 1).

Base-Pair Stacking. To help determine how base pairs of type C or D provide the unusual stability of the 2C duplex, two-dimensional (2D) NMR experiments were conducted. Resonances were assigned by standard NOESY and COSY routines (29). A full 2D NOESY plot (mixing time 300 ms) and a 1D spectrum of sequence 2C are shown in Fig. 3. Table 1 lists some important experimental NOE connectivities for sequence 2C and indicates predicted NOEs for right-handed duplexes with the same sequence as 2C but with mismatched G·A base pairs of type A or B. Although a full analysis of the 2D results is beyond the scope of this report, several key cross-peaks clearly characterize the duplex structure and the base-pair type for the G·A mismatches. The characteristic NOE pattern for a right-handed duplex appears in Table 1. Fig. 4 shows the base aromatic proton (H8/H6) to sugar H1′ proton fingerprint region of the NOESY spectrum and the sequential connections for a right-handed DNA. Except for the 5′ terminal base, each H6/H8 proton gives NOEs to its own and the H1′ proton of its 5′ neighbor residue, and except for the 3′ terminal sugar, each H1′ proton gives NOEs to its own and its 3′ successive H8/H6 protons. Also as expected for a right-handed duplex, C(6)H5 has NOE to G(5)H8 and the CH_3 groups of T(2) and T(10) have NOEs to the 5′ AH8 protons at A(1) and A(9), respectively (Table 1 and Fig. 3).

At a short mixing time (60 ms) in NOESY spectra, all the cross-peaks of H8/H6–H1′, including those of mismatched purines, disappear but the cross-peak of H6–H5 of C(6) can still be seen. The distance between CH6 and CH5 is 2.5 Å, and the distance between H8 and H1′ in the same nucleotide is 2.5 Å if the glycosidic angle is syn or 3.7 Å if it is anti (30). The much weaker NOE intensities of H8/H6–H1′ cross-peaks, relative to CH5–CH6, strongly suggest that all the nucleotides in sequence 2C adopt the anti conformation.

Also, at mixing times <60 ms in NOESY spectra, there are no observable cross-peaks in the region of H8/H6 to H3′ and only the cross-peaks from H6/H8 to H2′,H2″ protons are seen. With the bases in an anti conformation, the shorter distances from H8/H6 protons to H2′,H2″ protons than to H3′ protons indicate that the sugars adopt C2′-endo/C3′-exo conformations (29). This sugar conformation is confirmed by all resolved coupling patterns in COSY spectra, and it is particularly obvious for the well resolved signals of the two mismatched adenosines. For mismatched guanosines, however, a clear coupling pattern could not be obtained because of overlap of resonances in both the H1′ and H2′,H2″ regions.

A surprising result from NOESY data presented above is that in spite of its four G·A mismatch base pairs, sequence 2C is quite similar to a standard B-form duplex. The helix has standard right-handed connectivities; all bases are anti and the sugars are all in the C2′-endo conformational region. There are some unusual observations however. In a B-family duplex the chemical shifts of AH8 proton signals are downfield of AH2 signals, but they are reversed in the 2C duplex for A(4) and A(8). The A(4)H8 (7.34 ppm) and A(8)H8 (7.42 ppm) proton signals are significantly upfield of the A(4)H2 (7.91 ppm) and A(8)H2 (7.84 ppm) signals. Because of the unusual nature of these shifts they were confirmed by $^1H/^2H$ exchange experiments. As expected, GH8 protons exchanged rapidly, AH8 protons exchanged more slowly, and AH2 protons did not exchange.

The mismatched base stacking in the 2C duplex is defined by several NOEs at the G·A mismatches (X in Table 1). There

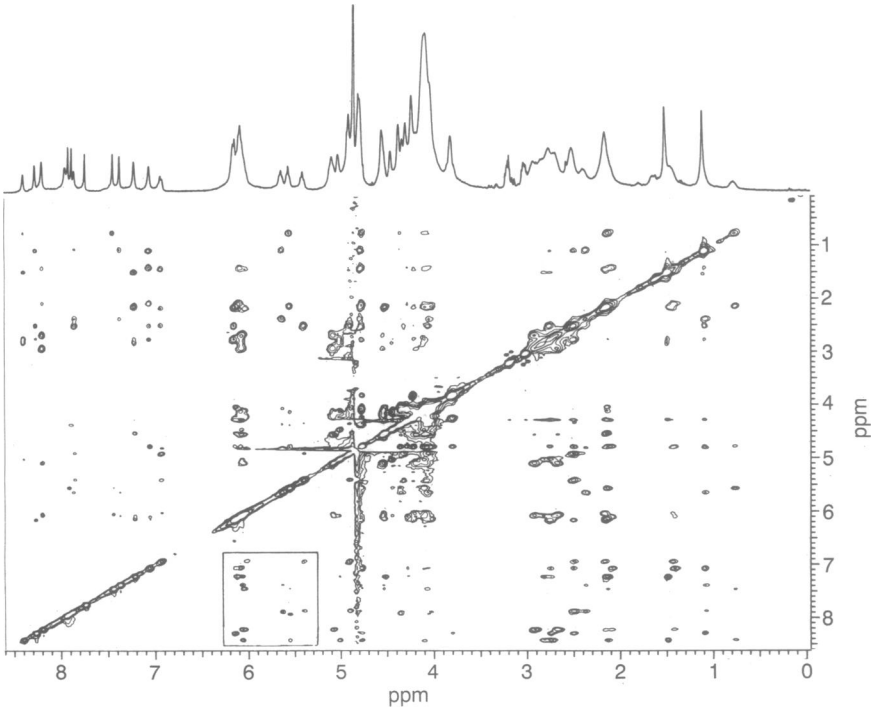

FIG. 3. 1D and 2D NOESY proton NMR spectra of sequence 2C-10 at 20°C. The sample was 3 mM in strands in ^2H_2O buffer containing 7.5 mM sodium phosphate, 0.2 mM NaCl, and 0.5 mM EDTA, pH 6.8. Sequences 2C and 2C-10 give very similar spectra and the 2C-10 spectrum is shown here for its better resolution and simplicity (10 versus 11 bases). The boxed area of the spectrum is expanded in Fig. 4.

Table 1. Critical NOE connectivities for the structure of 2C

		A1 H8	T2 H6	G3 H8	A4 H8	G5 H8	C6 H6	G7 H8	A8 H8	A9 H8	T10 H6	A1 H2	A4 H2	A8 H2	A9 H2		
A1	H1'	◆	◆													A1	H1'
T2	H1'		◆	◆												T2	H1'
G3	H1'			◆	◆											G3	H1'
A4	H1'				◆	◆								X		A4	H1'
G5	H1'					◆	◆									G5	H1'
C6	H1'						◆	◆								C6	H1'
G7	H1'							◆	◆							G7	H1'
A8	H1'								◆	◆			X			A8	H1'
A9	H1'									◆	◆					A9	H1'
T10	H1'										◆					T10	H1'
T2	CH_3	◆	◆													T2	CH_3
T10	CH_3									◆	◆					T10	CH_3
C6	H5					◆	◆									C6	H5
T2	NH3											◆			◆	T2	NH3
G3	NH1							X	B					A		G3	NH1
G5	NH1												A			G5	NH1
G7	NH1			X	B								A			G7	NH1
T10	NH3											◆			◆	T10	NH3

Distance dependent proton–proton through space interactions that are experimentally observed or expected for different conformations are shown. ◆, NOEs typical of a right-handed B-family duplex DNA that are seen in 2C; **A**, NOEs expected of a duplex with G·A pairs of type A that are not seen in 2C; **B**, NOEs expected of a duplex with G·A pairs of type B that are not seen in 2C; **X**, unusual NOEs that are observed in the 2C duplex.

are two strong H2 to H1′ cross-peaks corresponding to mismatched A(4)H2 to A(8)H1′ and A(8)H2 to A(4)H1′ (box in Fig. 4). The intensities of cross-peaks observed from A(4)H1′ to A(4)H8 and from A(8)H1′ to A(8)H8 are much weaker than those from A(4)H1′ to A(8)H2 and from A(8)H1′ to A(4)H2 (box in Fig. 4), and at shorter mixing times the latter exist but the former disappear. These reversed relative NOESY cross-peak intensities (28) indicate that the distances between A(4)H2 and A(8)H1′ and between A(8)H2 and A(4)H1′ are unusually short and, therefore, an unconventional base arrangement must exist. An A(4) over A(8) stacking from opposite strands in a pseudosymmetrical way with G·A base pairs of type C or D could give the observed strong NOEs of A(4)H2 to A(8)H1′ and A(8)H2 to A(4)H1′.

We also observed unusual cross-strand NOEs at G(3)H8 when G(7)NH1 (imino proton) was irradiated and at G(7)H8 when G(3)NH1 was irradiated in H_2O experiments (Table 1).

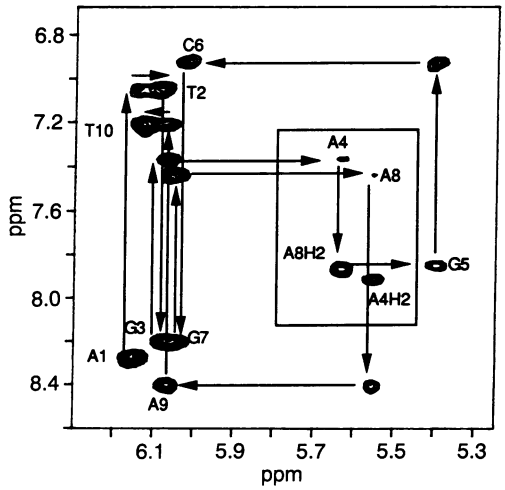

FIG. 4. Expanded plot of the aromatic to sugar H1′ region of the NOESY spectrum in Fig. 3. The H8/H6 protons and H1′ protons are connected through the lines in the typical manner for a right-handed duplex (29). The mismatched adenosines H8–H1′ and unusually strong H2–H1′ cross-peaks are shown in the box. As can be seen, the A(4)H8–A(4)H1′ and A(8)H8–A(8)H1′ cross-peaks are much weaker than the A(4)H2–A(8)H1′ and A(8)H2–A(4)H1′ cross-peaks.

G(3) and G(7) are located on opposite strands and, unless G(3) and G(7) stack over each other, it is impossible to give such symmetrical NOEs. We did not observe any NOEs from the mismatched GNH1 protons to partner AH2 or AH8 (A and B in Table 1) and this confirms that G·A pairs of type A or B are not formed.

In summary, the NMR results indicate that the proposed base-pairing scheme for sequence 2C is correct and suggest that the A(1)·T(10), T(2)·A(9), and G(5)·C(6) base pairs adopt conformations close to those expected for a standard B-family duplex. The G·A base pairs, however, must fit into the B-form duplex without any serious discontinuities and are paired as type C or D. The mismatches also have unusual stacking interactions with G(3) stacking over G(7) and A(4) over A(8).

Molecular Model. To determine whether a duplex could be constructed that obeyed the observed interactions from NMR studies, we built a model of the hexamer sequence 5′-d[A(1)T(2)G(3)A(4)G(5)C(6)]·5′-d[G(5)C(6)G(7)A(8)A(9)-T(10)], numbered as in sequence 2C, with the terminal two base pairs at each end of the duplex in Watson–Crick B-form type structures and the two central G·A in either type C or type D mismatch base pairs. Both were energy minimized. The hexamer duplexes with G·A pairs of type C were severely distorted due to steric clash at adjacent mismatched base pairs and duplexes containing these types of base pairs have relatively high energy. On the other hand G·A base pairs of type D can be fitted surprisingly well into a standard B-family duplex with all bases anti and all sugars in the C2′-endo region, and A(4) of the hexamer stacked over A(8) and G(3) over G(7). Fig. 5 shows a top view of the two mismatched G·A pairs from the minimized hexamer and this illustrates the cross-strand A–A and G–G stacking. The distance from each mismatched amino GN2 to the mismatched AN7 (Fig. 5) is ≈3 Å, a reasonable hydrogen bond distance (8). The distances between ANH_2 and GN7, however, are longer (N–N distances of 4.3 and 4.6 Å) than normal hydrogen bonds, but there are two extra potential hydrogen bonds between GNH_2 and the phosphate backbone (Fig. 5) to create bifurcated hydrogen bonds stabilizing this base-pairing conformation. The distances from each mismatched AH1′ to the other mismatched AH2 and from each mismatched GH8 to the other GNH1 (curved arrows in Fig. 5) are within 3.8 Å,

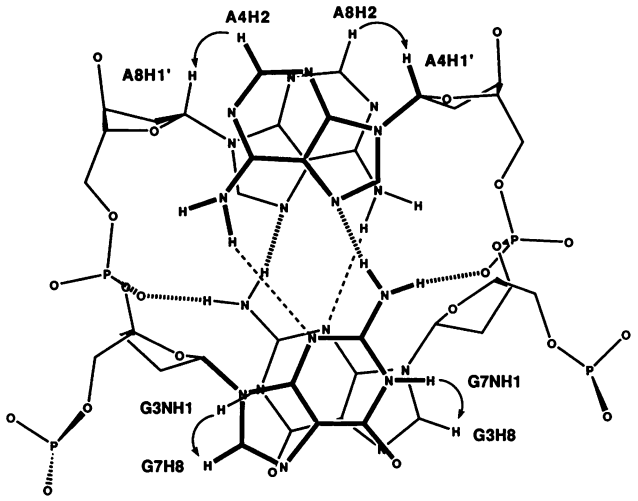

FIG. 5. Top view of the model for the G·A mismatched base pairs. The top G·A pair has thicker lines and the hydrogens on the backbones and at AH8 positions are deleted for clarity in visualizing the stacking interactions. The base-pairing hydrogen bonds, including the proposed extra hydrogen bonds between phosphate backbone oxygens and G-NH_2 (≈2.8 Å from N to O) are shown with dashed lines. Base pairing can be visualized by comparison with the type D model in Fig. 1. Critical NOEs (X in Table 1), predicted by this model, are shown with curved arrows.

consistent with NOE results. All standard B-form NOEs (Table 1) are predicted by the model. The mismatched AH8 protons are inside the purine shielding range, explaining their upfield resonances. The molecular modeling results, thus, strongly suggest that all the G·A mismatches in sequence 2C are a modification of type D and stack with a pattern of adenosine over adenosine and guanosine over guanosine.

Structural changes and the lack of one hydrogen bond make duplexes with G·A mismatches generally less stable than similar Watson–Crick duplexes with G·C base pairs (13, 16). Four G·A mismatches in a 10-base-pair duplex should destabilize sequence 2C considerably, but the energies from minimization of a model for 2C [5′-d(ATGAGC)$_2$, −489 kJ/mol] and a sequence related Watson–Crick duplex [5′-d(ATGAGC)·5′-d(GCTCAT), −449 kJ/mol] are similar. This similarity indicates that the excellent purine–purine stacking of the two adjacent G·A mismatches (Fig. 5) makes a major contribution toward the 2C duplex stability.

Conclusions. We have discovered a B-form helix with unusual base stacking and type D G·A base pairs. The adjacent purine mismatches with sequence 5′-GA-3′ fit into a standard B-form duplex with little distortion. The mismatches are stabilized by very efficient purine–purine stacking and by hydrogen bonding. In addition to demonstrating another B-type DNA conformation the observation of unusual stability and conformation of 5′-GA-3′ mismatches is important for several reasons. For example, the conserved sequences in the consensus active site region of hammerhead ribozymes contain 5′-GA-3′ residues that are adjacent to helix II of the hammerhead (see refs. 31–33) and are capable of forming type D base pairs. Base pairs of type D leave functional groups such as the keto and imino groups of guanosine and N3 of adenosine accessible for tertiary interactions or for use as part of the nuclease activity of ribozymes.

Turner and coworkers (34) have found that RNA oligomers containing adjacent 5′-GA-3′ mismatches are more stable than those with 5′-AG-3′ mismatches. In addition, the 5′-AG-3′ mismatches have imino protons in the expected region while the 5′-GA-3′ sequence does not. We have also found with DNA that 5′-AG-3′ mismatch sequences are significantly less stable than the 5′-GA-3′ sequence (unpublished data). These observations point to a critical sequence dependence for the unusual mismatched conformation of sequence 2C and strongly suggest that such a stacking arrangement can also occur in RNA, perhaps in such critical regions as the ribozyme active site. Orbons *et al.* (15), with 5′-d(CGCGAGCG), have observed G·A mismatched base pairs with many chemical shifts similar to the base pairs in 2C. Although they did not propose base pairing of the type observed in 2C, we feel that such pairing best explains their results.

The highly polymorphic nature of DNA has now been demonstrated in many cases but the 2C duplex provides an unparalleled example of the ability of the double helix to adopt a wide range of local conformational variations and quickly return to a standard B-form conformation.

We thank Dr. Turner for sending us a preprint of his work on RNA G·A mismatch base pairs and for helpful discussions on mismatched base pairs. This work was supported by National Institute of Allergy and Infectious Diseases Grant AI-27196 and by a National Science Foundation equipment grant for the Varian VXR-400.

1. Blackburn, E. H. & Szostak, J. W. (1984) *Annu. Rev. Biochem.* **53**, 163–194.
2. Henderson, E., Hardin, C. C., Walk, S. K., Tinoco, I. & Blackburn, E. H. (1987) *Cell* **51**, 899–908.
3. Radman, M. & Wagner, R. (1984) *Curr. Top. Microbiol. Immun.* **108**, 23–28.
4. Topal, M. D. & Fresco, J. R. (1976) *Nature (London)* **263**, 285–289.
5. Friedberg, E. C. (1985) *DNA Repair* (Freeman, New York).
6. Kramer, B., Kramer, W. & Fritz, H.-J. (1984) *Cell* **38**, 879–887.
7. Fazakerley, G. V., Quinard, E., Woisard, A., Guschlbauer, W., van der Marel, G. A., van Boom, J. H., Jones, M. & Radman, M. (1986) *EMBO J.* **5**, 3697–3703.
8. Saenger, W. (1984) *Principles of Nucleic Acid Structure* (Springer, New York).
9. Traud, W. & Sussman, J. L. (1982) *Nucleic Acids Res.* **10**, 2701–2708.
10. Kim, S. H. (1981) *Topics in Nucleic Acid Structure*, ed. Neidle, S. (Halsted, London), pp. 83–112.
11. Noller, H. F. (1984) *Annu. Rev. Biochem.* **53**, 119–162.
12. Dodgson, J. B. & Well, R. D. (1977) *Biochemistry* **16**, 2374–2379.
13. Aboul-ela, F., Koh, D., Martin, F. H. & Tinoco, I. (1985) *Nucleic Acids Res.* **13**, 4811–4824.
14. Poltev, V. I. & Shulyupina, N. V. (1986) *J. Biomol. Struct. Dyn.* **3**, 739–765.
15. Orbons, L. P. M., van der Marel, G. A., van Boom, J. H. & Altona, C. (1987) *J. Biomol. Struct. Dyn.* **4**, 939–963.
16. Patel, D. F., Kozlowski, S. A., Ikuta, S. & Itakura, K. (1984) *Biochemistry* **23**, 3207–3217.
17. Kan, L. S., Chandrasegaran, S., Pulford, S. M. & Miller, P. S. (1983) *Proc. Natl. Acad. Sci. USA* **80**, 4263–4265.
18. Prive, G. G., Heinemann, U., Chandrasegaran, S., Kan, L. S., Kopka, M. L. & Dickerson, R. E. (1987) *Science* **238**, 498–504.
19. Gao, X. & Patel, D. J. (1989) *J. Am. Chem. Soc.* **110**, 5178–5182.
20. Hunter, W. N., Brown, T. & Kennard, O. (1986) *J. Biomol. Struct. Dyn.* **4**, 173–191.
21. Chang, E. H., Yu, Z., Shinokuza, K., Zon, G., Wilson, W. D. & Strekowska, A. (1989) *Anti-Cancer Drug Des.* **4**, 221–232.
22. Wilson, W. D., Dotrong, M. H., Zuo, E. T. & Zon, G. (1988) *Nucleic Acids Res.* **16**, 5137–5151.
23. Hore, P. J. (1983) *J. Magn. Reson.* **55**, 283–300.
24. Mohamadi, F., Richards, N. G. J., Guida, W. C., Liskamp, R., Lipton, M., Caufield, C., Chang, G., Hendrickson, T. & Still, W. C. (1990) *J. Comput. Chem.* **11**, 440–467.
25. Weiner, S. J., Kollman, P. A., Nguyen, D. T. & Case, D. A. (1986) *J. Comput. Chem.* **7**, 230–252.
26. Cantor, C. R. & Schimmel, R. R. (1980) *Biophysical Chemistry* (Freeman, San Francisco).
27. Kearns, D. R. (1977) *Annu. Rev. Bioeng.* **6**, 477–523.
28. Uesugi, S., Oda, Y., Ikehara, M., Kawase, Y. & Ohtsuka, E. (1987) *J. Biol. Chem.* **262**, 6965–6968.
29. Wuthrich, K. (1986) *NMR of Proteins and Nucleic Acids* (Wiley, New York), p. 235.
30. Patel, D. J., Kozlowski, S. A., Nordheim, A. & Rich, A. (1982) *Proc. Natl. Acad. Sci. USA* **79**, 1413–1417.
31. Keese, P. & Symons, R. H. (1987) *Viroids and Viroid-like Pathogens* (CRC, Boca Raton, FL), pp. 1–47.
32. Ruffner, D. E., Dahm, S. C. & Uhlenbeck, O. C. (1989) *Gene* **82**, 31–41.
33. Heus, H. A., Uhlenbeck, O. C. & Pardi, A. (1990) *Nucleic Acids Res.* **18**, 1103–1108.
34. SantaLucia, J. J., Kierzek, R. & Turner, D. H. (1990) *Biochemistry* **29**, 8813–8819.